Moroccan Journal
of Chemistry
ISSN : 2351-812X


Mor. J. Chem., 2023, Volume 11, Issue 01, Page 61-76
https://revues.imist.ma/index.php/morjchem

# Effects of temperature, time and alkaline solution content on the mechanical properties of Class C fly ash-based geopolymer using Taguchi method

**Moutaoukil G.[1]*, Alehyen S.[1], Sobrados I. [2], Fadil M. [1], Taibi M. [1]**

[1]*Mohammed V University in Rabat, Centre Sciences des Matériaux, Laboratoire de Physico-Chimie des Matériaux Inorganiques et Organiques (LPCMIO), Ecole Normale Supérieure (E.N.S), Avenue Mohamed Bel Hassan El Ouazzani, BP 5118, Takaddoum-Rabat, Morocco.*
[2]*Instituto de Ciencia de Materiales de Madrid, Consejo Superior de Investigaciones Científicas (CSIC), C/Sor Juana Inés de la Cruz, 3, ES, 28049 Madrid, Spain*
**Corresponding author, Email address: ghizlane.moutaoukil9@gmail.com, ghizlane.moutaoukil@um5s.net.ma*

*Received 04 Nov 2022,*
*Revised 23 Dec 2022,*
*Accepted 25 Dec 2022*

*Citation: Moutaoukil G., Alehyen S., Sobrados I., Fadel M. and Taibi M. (2023) Effects of temperature, time and alkaline solution content on the mechanical properties of Class C fly ash-based geopolymer using Taguchi method, Mor. J. Chem., 14(1), 61-76. Doi: https://doi.org/10.48317/IMIST.PRSM/morjchem-v11i1.36838*

**Abstract:** This research aims to investigate the effects of three factors on the compressive strength of fly ash-based geopolymers by using the Taguchi method. The three studied factors include curing time, curing temperature and the percentages of NaOH and KOH in the alkaline solution. X-ray fluorescence spectrometry (XRF), Fourier Transform Infrared spectroscopy (FT-IR) spectroscopy, X-ray diffraction (XRD), Scanning electron microscopy (SEM) and mechanical tests were applied for characterization of raw materials and geopolymers samples. The results of the analysis have shown that the highest compressive strength achieved was 13.58 MPa and the optimum curing temperature, curing time and alkaline solution content were determined as 70°C, 24h and a mix of 50% NaOH/ 50% KOH respectively.

**Keywords:** geopolymer ; fly ash ; compressive strength ; Taguchi method.

## 1. Introduction

The development of knowledge on geopolymer technology tends to show that they could potentially offer an efficient and ecological alternative to ordinary Portland cement (OPC). Geopolymers are inorganic polymers produced by reacting a pozzolanic source (blast furnace slag, metakaolin, fly ash and pozzolan, etc.) with an aqueous solution of alkali hydroxide and/or alkali silicate. The geopolymerization reaction approach is different from the pozzolanic reaction. For pozzolanic cement, the resistance gain depends mainly on the presence of calcium to form calcium silicate hydrates (CSH) while for geopolymers, it depends on the poly-condensation reaction between a pozzolanic material containing silica and alumina with an alkaline activator to form an aluminosilicate (Na, K) –A-S-H gel which is the main binding phase in the geopolymer matrix (van Jaarsveld *et al*., 2002).

The geopolymers properties depend upon the nature of the raw materials and the preparation conditions (Monsif et al., 2017). A lot of works have been done studying the effects of the initial conditions of synthesis such as the curing time and temperature (Hardjito *et al*., 2004; Rattanasak and

Chindaprasirt, 2009; Riahi *et al*., 2012; Soutsos *et al*., 2016), the NaOH concentration and the nature of the alkaline activator used (Kaur *et al*., 2018; Nmiri *et al*., 2017; Olivia and Nikraz, 2012) as well as the paparticles size (Assi *et al*., 2018). The determination of the optimum synthesis parameters allows the production of geopolymer with high compressive strength in less time and with less raw material and energy consumption.

Taguchi's design offers a systematic approach for optimizing various parameters. It is a suitable experimental design that allows the evaluation of the effects of several parameters to be studied simultaneously with a minimum number of experiments. Chemical attack damage to high-strength concrete mixtures prepared with silica fume (SF) and blast furnace slag (BFS) was studied by Turkmen *et al* (Türkmen *et al*., 2008). They used the "Taguchi method" to specify the optimal conditions for obtaining the most durable concrete mixtures (Türkmen *et al*., 2008). An optimization of fly ash geopolymer blends using the Taguchi method was carried out by Monita *et al*. They studied both the mechanical properties and durability of the optimal mixtures (Olivia and Nikraz, 2012). Nazari *et al* investigated the design of geopolymers produced by Portland cement as an aluminosilicate source using the Taguchi method (Nazari *et al*., 2012). Riahi et al have optimized the compressive strengths of fly ash-based geopolymers at 2 and 7 days of curing using the Taguchi method by taking into account three main formulation parameters namely the curing temperature, the curing time and the concentration of sodium hydroxide (NaOH) (Riahi *et al*., 2012). In order to design optimal mixing ratios for geopolymer concrete Hadi *et al*. used ground granulated blast furnace slag (GGBFS) as a source of aluminosilicate, which is hardened under ambient conditions (Hadi *et al*., 2017). The main design parameters studied were the content of binder, the ratio of alkaline activator to binder content, the ratio of sodium silicate to sodium hydroxide and the concentration of sodium hydroxide (Hadi *et al*., 2017).

The purpose of this paper is to investigate the effect of curing time, curing temperature and alkaline solution nature (Na/K) on the mechanical and microstructural of the fly ash-based geopolymers. For this purpose, the statistical Taguchi method was used to design and analyze the experimental results obtained. The ANOVA method was employed to examine the obtained results in order to determine the optimum level for each factor.

## 2. Methodology

### *2.1 Materials*

Fly ash used as raw materials was supplied from the thermal coal plant of Jorf Lasfar in Morocco; it's classified as class C according to ASTM C618-08a specification. The main oxide composition of fly ash is reported in **Table 1** according to X-ray fluorescence analysis (XRF). The alkaline activators used in the preparation of the geopolymer were $Na_2SiO_3$ sodium silicate solution (18% $Na_2O$ and 63% $SiO_2$), KOH potassium hydroxide pellets (purity >97%) and NaOH sodium hydroxide pellets (purity >97%).

**Table 1: Chemical composition of Fly Ash**

| ***Constituent*** | **LOI** | **$SiO_2$** | **$Al_2O_3$** | **$Fe_2O_3$** | **CaO** | **$K_2O$** | **$Na_2O$** | **$TiO_2$** | **$SO_3$** | **$P_2O_5$** |
|---|---|---|---|---|---|---|---|---|---|---|
| *%* | 7.12 | 30.59 | 15.05 | 4.25 | 32.99 | 2.08 | 7.4 | 1.51 | 2.66 | 0.90 |
| ***Constituent*** | **MgO** | **Rb** | **SrO** | **BaO** | **MnO** | | | | | |
| *%* | 2.5 | 0.0694 | 0.20 | 0.12 | 0.10 | | | | | |

LOI: loss of ignition

*2.2 Method*

***2.2.1 Design of experiments using the Taguchi method***

- Optimized Factors:

The three factors that were considered for Taguchi's experimental design were the curing temperature, oven curing time, and the percentages of NaOH and KOH in the alkaline solution, each at 3 levels. The three studied factors, containing three levels of each one, are reported in **Table 2**.

**Table 2: Boundaries of factors**

| | Factor | Unit | levels 1 | 2 | 3 |
|---|---|---|---|---|---|
| X1 | Curing time | h | 8 | 12 | 24 |
| X2 | Curing Temperature | °C | 25 | 40 | 70 |
| X3 | Alkaline solution | - | 100%NaOH | 50%NaOH | 100%KOH |

- Response: compressive strength of 28 days.
- Experimental matrix:

Three parameters, at three levels each, would give 27 experiments in the full factorial design ($3^3$). However, Taguchi gave only nine experimental runs using the L9 orthogonal array as shown in the matrix of experience (**Table 3**) and the experimental design (**Table 4**).

**Table 3: matrix of the 9 experiments generated by the Taguchi method**

| Experience number | X1 | X2 | X3 |
|---|---|---|---|
| 1 | 1 | 1 | 1 |
| 2 | 1 | 2 | 2 |
| 3 | 1 | 3 | 3 |
| 4 | 2 | 1 | 2 |
| 5 | 2 | 2 | 3 |
| 6 | 2 | 3 | 1 |
| 7 | 3 | 1 | 3 |
| 8 | 3 | 2 | 1 |
| 9 | 3 | 3 | 2 |

**Table 4: The experimental design of the nine experiments**

| | *Curing time (h)* | *Curing Temperature (°C)* | *Alkaline solution* |
|---|---|---|---|
| GP1 | 8 | 25 | 100%NaOH |
| GP2 | 8 | 40 | 50%NaOH & 50% KOH |
| GP3 | 8 | 70 | 100%KOH |
| GP4 | 12 | 25 | 50%NaOH & 50% KOH |
| GP5 | 12 | 40 | 100%KOH |
| GP6 | 12 | 70 | 100%NaOH |
| GP7 | 24 | 25 | 100%KOH |
| GP8 | 24 | 40 | 100%NaOH |
| GP9 | 24 | 70 | 50%NaOH & 50% KOH |

- Statistical analysis

Fitted model significance was tested using the ANOVA test by calculating the $Fratio_{(MSR/MSr)}$, the ratio of the mean square due to regression (MSR) to the residual mean square (MSr). To accept or reject the significance of each factor at the 95% significance level, t-students were used. The t-student tests for each factor were paired with p-value tests that are defined as the lowest level of significance to reject a null hypothesis (Fadil et al., 2018). The generation of the Taguchi experiment design, the statistical data analysis and the optimization step were performed using Minitab 18.

### *2.2.2 Sample preparation*

In order to prepare the alkaline solution, pellets of sodium hydroxide and/or potassium hydroxide were diluted in distilled water to a concentration of 12M; then added to the sodium silicate. The ratio of $NaOH/Na_2SiO_4$ was 2.5. In addition, the liquid/solid (L/S) ratio was set as 0.4.

The preparation of the geopolymer samples was conducted according to the design of the mixtures suggested by the Taguchi method. Thereafter, the geopolymer pastes were filled into the moulds and placed in an electric oven at the specified curing temperature. After the curing period, the samples were allowed to air dry in the laboratory until the day of testing. The compositions of the synthesized fly ash geopolymer were reported in **Table 5.**

**Table 5: Composition of synthesized geopolymer samples**

| | FA | NaOH | KOH | $Na_2SiO_3$ |
|---|---|---|---|---|
| GP1<br>GP6<br>GP8 | 100 | 11.43 | 0 | 28.57 |
| GP2<br>GP4<br>GP9 | 100 | 5.71 | 5.71 | 28.57 |
| GP3<br>GP5<br>GP7 | 100 | 0 | 11.43 | 28.57 |

### *2.3 Product characterisation*

The compressive strength was measured in geopolymer pastes after 7 and 28 days of curing, where three cylinders (35*70 $mm^3$) were tested in an automatic pressure testing machine YAW-300 according to ASTM C39 standard. The morphology of the products was examined using an FEI quanta 450 FEG scanning electron microscope. Samples were examined in cross-section and were coated with gold or palladium prior to measurement to avoid charge accumulation on the surface of the sample and to reduce the depth of beam penetration, thus improving the image. FTIR spectroscopy measurements were performed on a VERTEX 70 instrument in MIR transmission mode with eight scans per sample, in the 4000 $cm^{-1}$ to 400 $cm^{-1}$ wavenumber range with a resolution of 4 $cm^{-1}$. X-ray diffraction was used to study the phase distribution of the powders on an Xpert-Pro diffractometer. The data were collected in a 2θ range from 10 to 70° with a step size of 0.02° using Cu Kα1 radiation (λ = 1.54056 Å).

## 3. Results and Discussion

### 3.1 Mechanical and microstructural characterization

#### a. Mechanical properties

Compressive strength at 7 and 28 days was used as the evaluation criteria for the nine mixtures according to the Taguchi method. **Fig. 1** shows the increase of compressive strength from 7 to 28 days of curing. According to this figure, the highest strength is achieved by the sample GP9, which has been cured in an oven for 24 hours at 70°C with an alkaline solution content of 50% NaOH and 50% KOH. On the other hand, the lowest strength is related to the sample GP4 which has been cured in an oven for 12 hours at 25°C with an alkaline solution content of 50% NaOH and 50% KOH.

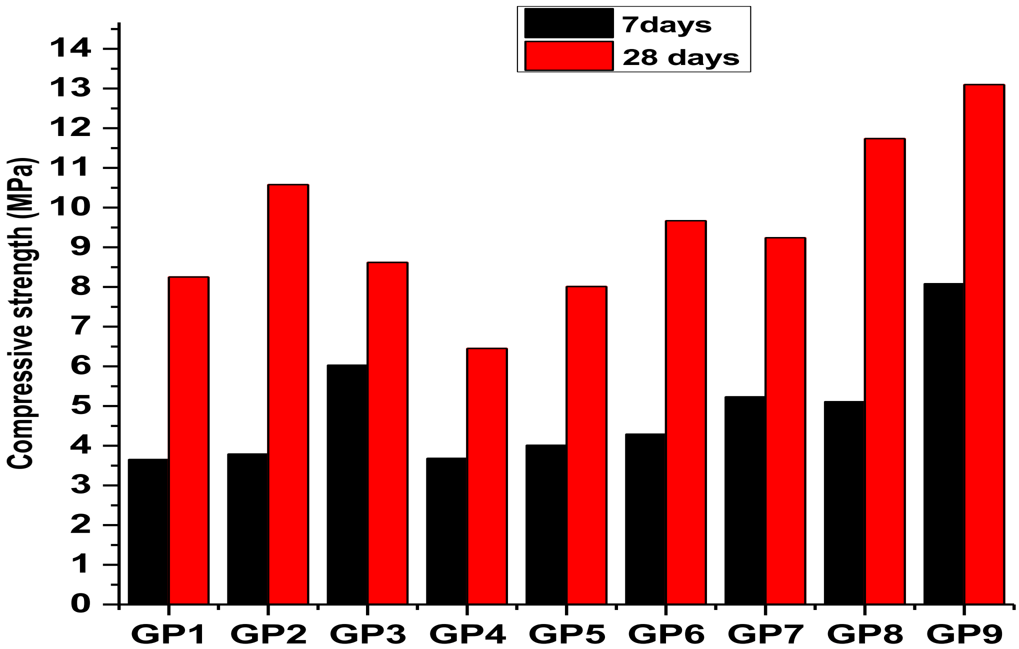


**Fig. 1: Compressive strength of the geopolymer specimens after 7 and 28 curing days.**

The obtained compressive strength values for the synthesized geopolymers are relatively low. Indeed, the compressive strengths of fly ash-based geopolymers are in a range of several MPa to over 100 MPa, depending on chemical composition, curing temperature, curing time, and raw material sources. In addition, the compressive strengths of geopolymers are also affected by water content, alkali activators nature and content, and curing humidity. Criado *et al*. carried out the synthesis of fly ash-based geopolymers using a $Na_2O/SiO_2$ ratio of 1/0.69 at a temperature of 85°C and obtained compressive strength values of 55MPa and 95MPa after 7 and 180 days of curing respectively (Criado *et al*., 2005); de Vargas *et al*. synthesized fly ash-based geopolymers with a $Na_2O$ / $SiO_2$ ratio of 0.4 at a temperature of 80°C and obtained compressive strength values of 5.3 MPa and 21.3MPa after 7 and 180 hardening days respectively (de Vargas *et al*., 2011); Fletcher *et al*. used natural aluminosilicate materials to synthesize geopolymers at 90°C overnight with a compressive strength value of 10.9 MPa (Fletcher *et al*., 2005).

**Fig. 2** displayed the evolution of compressive strengths at 7 and 28curing days respectively as a function of temperature for different KOH and NaOH content. It is noted that the highest compressive strengths are obtained for curing temperatures of 70°C. In fact, the reaction kinetics of

geopolymerization are influenced by the curing temperature and as a consequence of the evolution of the mechanical performance of geopolymers.

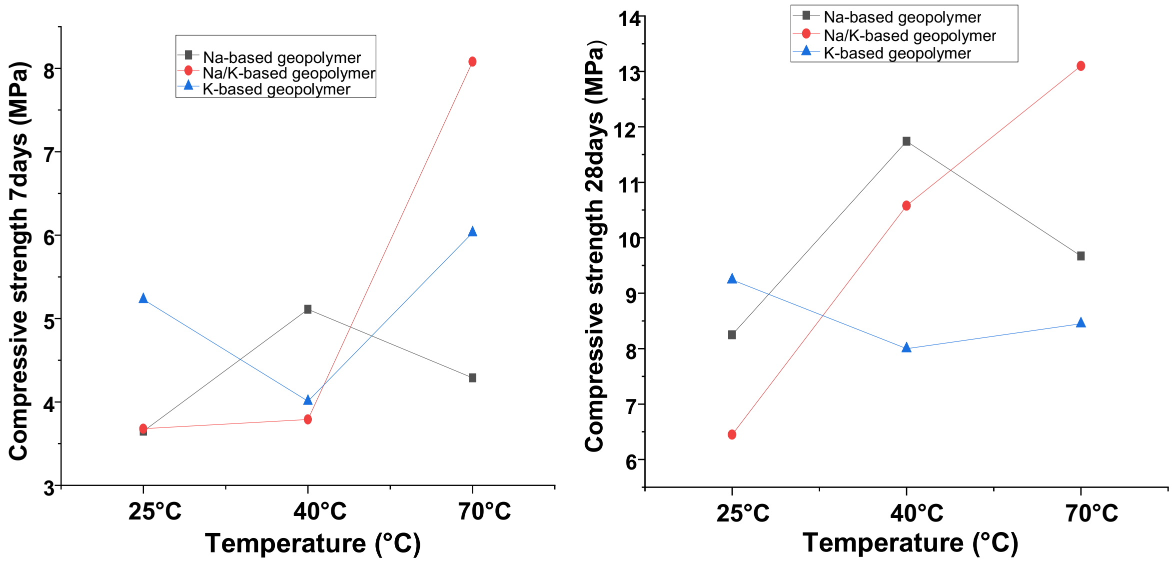


(a) (b)

**Fig. 2:** compressive strength of 7 days (a) and 28days (b) vs temperature for different Na, K and Na/K based geopolymers

At elevated temperatures, the geopolymerization reaction is accelerated, producing higher quantities of reactive monomeric species of silica and alumina, which form the aluminosilicate gel by polycondensation, thus leading to the development of the mechanical resistance of the geopolymers (Görhan and Kürklü, 2014; Siyal *et al.*, 2016). However, in some cases, it has been observed that increasing the curing temperature above 75°C decreases the compressive strengths (Nazari *et al.*, 2011). A study of the effect of curing temperature on the geopolymerization of metakaolin-based geopolymers was carried out by Mo Bing –hui *et al* (Mo *et al.*, 2014). The optimal curing temperature of the geopolymer was found to be about 60°C, at which the geopolymer samples showed the best mechanical properties with a compressive strength of 97.95 MPa after 7 days of curing (Mo *et al.*, 2014). The curing temperature has been reported by Palomo *et al*. (Palomo *et al.*, 1999) as a reaction accelerator in fly ash-based geopolymers. J. Temuujin *et al*. (Temuujin *et al.*, 2009) stated that curing temperatures between 40°C and 80°C for 4 to 48 hours is one of the main conditions for geopolymer synthesis. In addition, Skvara *et al*. (Škvára et al., 2009) found that the reaction degree of class F fly ash-based geopolymeric system at 20°C for 70 days is equivalent to that at 60°C for 1 day. Contrariwise, it was reported by Hardjito *et al*.(Hardjito et al., 2008) that increased curing temperature doesn't always result in improved mecanicals properties of the material.

According to **Fig. 3**, the highest compressive strengths are obtained for a curing time of 24 h. This result is in agreement with the works of Gorhan *et al* (Görhan and Kürklü, 2014) and Hardjito *et al* (Hardjito *et al.*, 2002). These authors have all found that the optimal curing time for geopolymers is 24 h. However, Nazari *et al* (Nazari et *al.*, 2012) and Riahi *et al* (Riahi *et al.*, 2012) have noticed that the hardening time does not have much influence on the mechanical strengths. From

**Fig. 2** and **Fig. 3**, it is observed that the highest compressive strengths are obtained for activating solutions containing 50% NaOH and 50% KOH for the curing temperature of 70°C and curing time of

24h. Same results reported by Bouguermouh *et al.*, they found the highest compressive strength for samples containing a mix of NaOH and KOH (Bouguermouh *et al.*, 2017). The alkali metal cations play an important role in the geopolymerization process. The alkaline solution, which is the main source of alkaline cations, is essential for dissolving the reactive silicate and aluminate tetrahedra in the raw material.

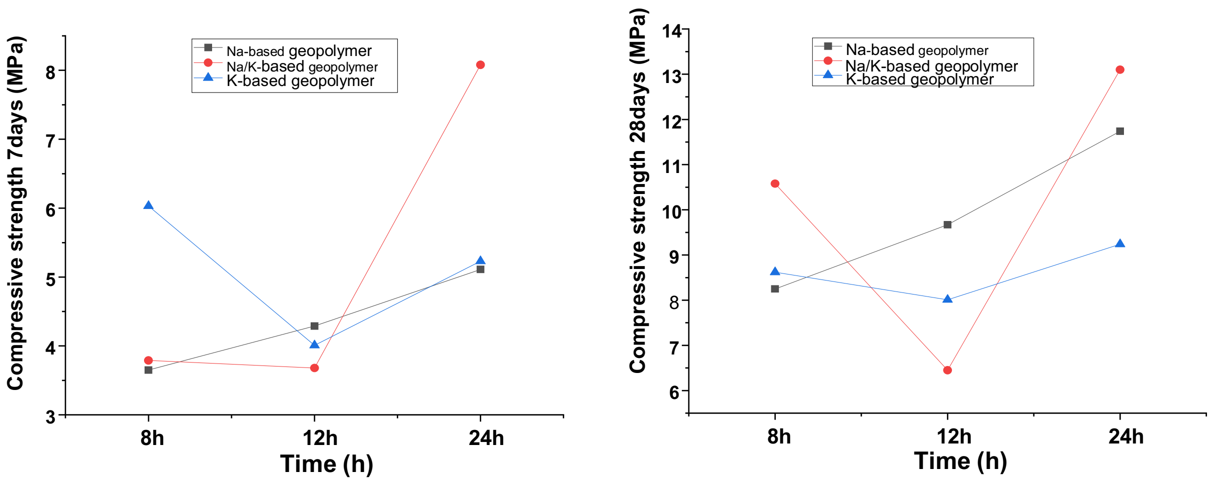


(c) (d)

**Fig. 3:** compressive strength at 7 days (c) and 28 days (d) vs curing time for different Na, K and Na/K based geopolymers

Several studies carried out to study the effect of alkaline activators have found that the mechanical properties of geopolymers are affected by the nature of the alkaline cation used. Geopolymers formulated with NaOH as an alkaline activator exhibit better compressive strength compared to those formulated with KOH (Abdul Rahim *et al.*, 2014; Hosan *et al., 2016; Leong et al., 2016)*. Xu and Deventer (Xu and Van Deventer, 2000) explained the fact that the compressive strengths of geopolymers based on NaOH are higher than those formulated on KOH by the acceleration of the dissolution step of the geopolymerization reaction initiated by $Na^+$ ions ( van Jaarsveld et *al.*, 2003). Furthermore, K+ based geopolymers have been reported to have a higher compressive strength (Xu *et al.*, 2001; Xu and van Deventer, 2003; Yao *et al.*, 2009). For example, with the presence of K+, it was reported by Xu et a (Xu and van Deventer, 2003) that an increase in the quantity of disorder in the gel phase formed as a result of increased compressive strength of geopolymers. The smaller ionic size of $Na^+$ (0.97) than the ionic size of $K^+$ (1.33 Å) activates the dissolution step of geopolymerization while $K^+$ is found under the same conditions affect the crystal morphology as the degree of condensation is higher in the presence of K compared to Na (van Jaarsveld and van Deventer, 1999).

### b. FA and Geopolymers characterization:

In order to perform the microstructural analysis, we selected GP9 with high compressive strength and GP4 which had the lowest strength value.

#### i. Fourier Transform InfraRed spectroscopy analysis (FTIR):

The infrared spectroscopic results for the fly ash, the low sample (GP4) and the optimal sample (GP9) are displayed in Fig. 4 and the assignment of the bands observed is presented in Table 6. The IR spectrum of the fly ash shows a distinct intensity band at 428 $cm^{-1}$ associated with the Si-O-Si bending

vibration and another intense band at 866 $cm^{-1}$ associated with the asymmetric stretching Si-O-Si and Si-O-Al vibration (Alouani and S. Alehyen, 2019; Lee and van Deventer, 2002). The band at 1041 $cm^{-1}$ due to asymmetric Si-O-Si and Al-O-Si stretching in the fly ash moves to lower frequencies (984$cm^{-1}$). This shift is an indication of the formation of aluminosilicate gel which is the main binding phase of the geopolymer matrix (Hamidi *et al*., 2016).

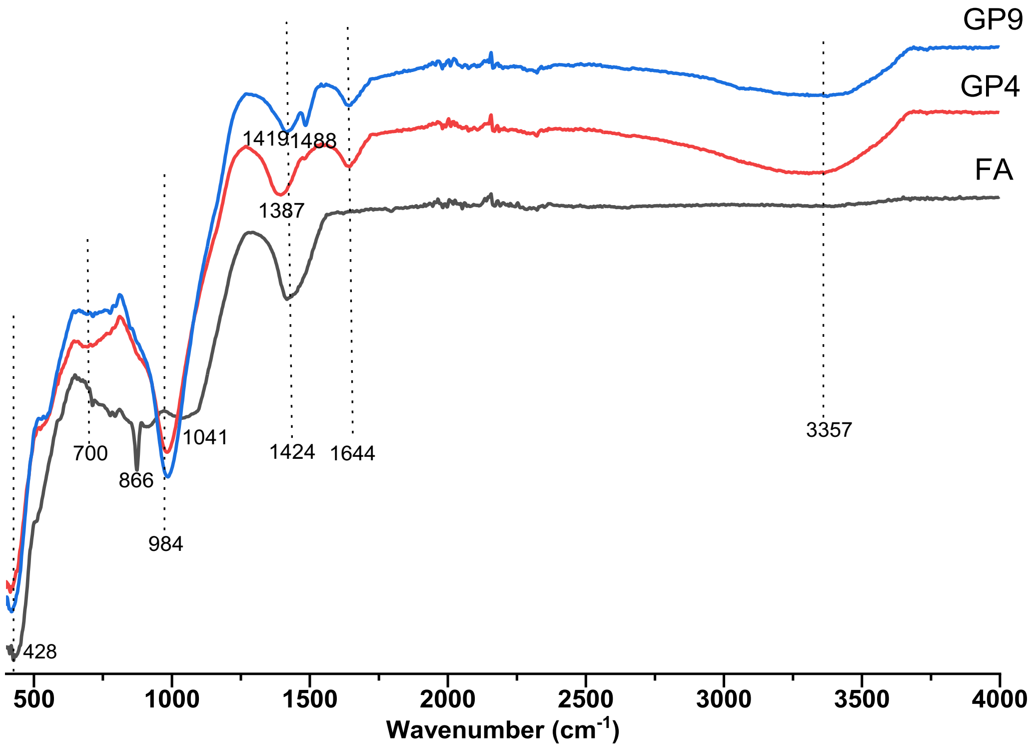


**Fig. 4: IR spectra of FA, the optimum (GP9) and the weak (GP4) samples.**

**Table 6: IR bands of fly ash and geopolymer samples (GP4 and GP9) with their possible assignments**

| *Samples* | *Wavenumbers ($cm^{-1}$)* | *Assignment* |
|---|---|---|
| FA | 428 | Si-O-Si bending vibration |
| | 700 & 866 | Al-O bending vibration |
| | 866 | asymmetric stretching Si-O-Si and Si-O-Al vibration |
| | 1041 | asymmetric Si-O-Si and Al-O-Si stretching |
| | 1424 | O-C-O streching( Carbonates) |
| GP4 | 984 | asymmetric Si-O-Si and Al-O-Si stretching |
| | 1387 | O-C-O stretching (Carbonates) |
| | 1644 | bending (H-O-H) vibrations |
| | 3357 | stretching (-OH) vibrations |
| GP9 | 984 | asymmetric Si-O-Si and Al-O-Si stretching |
| | 1419 & 1488 | O-C-O stretching (Carbonates) |
| | 1644 | bending (H-O-H) vibrations |
| | 3357 | stretching (-OH) vibrations |

The intensity of this band being higher for the GP9 sample than GP4 indicates the formation of more aluminosilicate gel in the geopolymer GP9. This fact explains the high compressive strength obtained for the sample GP9. The bands observed at 1644 and 3357 $cm^{-1}$ in the geopolymer samples are attributed to bending (H-O-H) and stretching (-OH) vibrations, respectively. The presence of these bands indicates the presence of bound water molecules (Zhang *et al*., 2012). These two bands are intense for the GP4 sample because it was cured at room temperature which explains the low mechanical resistance of this sample. Detailed study for the microstructural changes occurred in our samples can be found in the previous published paper (Moutaoukil *et al*., 2022).

### ii. X-Ray diffraction

**Fig. 5** shows the X-Ray diffraction spectra of fly ash, optimal and weak geopolymer samples. In the XR diffraction spectrum of fly ash, we can see that it consists of crystalline phases (quartz and mullite) and a large halo between 15° and 35° which characterizes the amorphous phase (Alehyen *et al*., 2017). a shift of the large halos between 20 and 40° can be remarked for the optimal geopolymer as well as for the weak geopolymer, which is attributed to the amorphous aluminosilicate gel. The presence of quartz and mullite peaks in the pattern can be explained by the incomplete geopolymerization reaction due to undissolved crystalline phases in the alkaline solution (Hadrami *et al*., 2020).

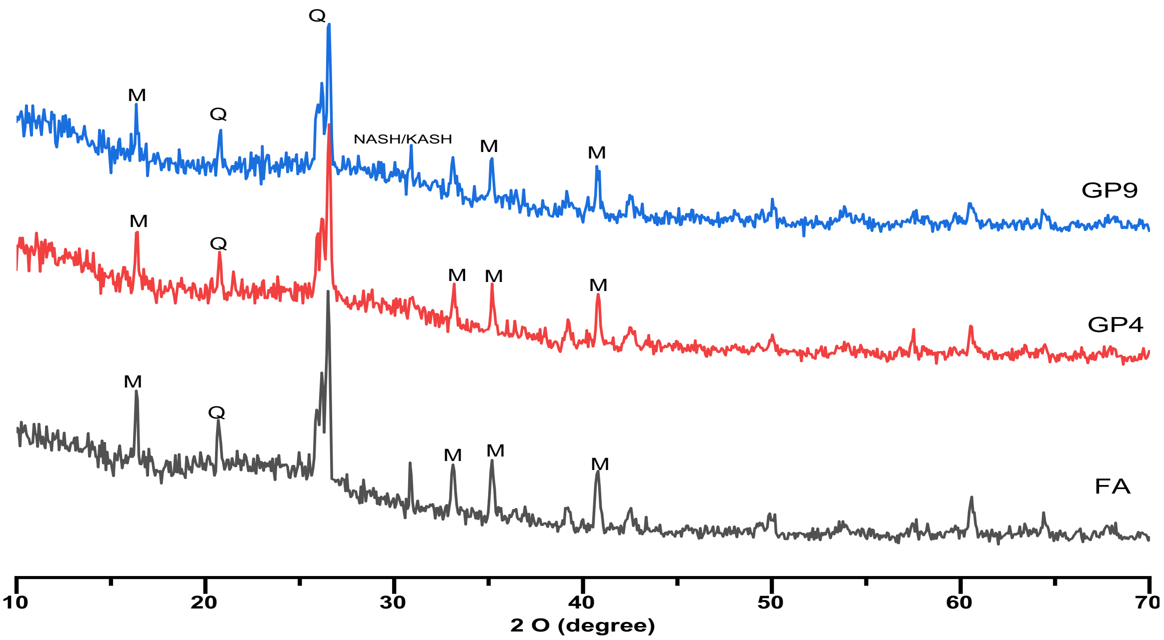


**Fig. 5: XRD pattern of FA, the optimum (GP9) and the weak (GP4) samples**

### iii. Scanning Electron Microscopy

The sample that recorded the highest compressive strength (GP9) and the sample that recorded lower compressive strength (GP4) were further analyzed using SEM and the micrographs resulting are shown in **Fig. 6**. Differences in morphologies of fly ash geopolymer samples were assessed for porosity, homogeneity and microcracks. The SEM micrographs of (GP9) reveal compact and denser structures which explain its high strength, there is also the crystal structure that is in a well-structured form which contributes to obtaining high compressive strength. The sample GP4 contain voids, microcracks and unreacted FA particles which results in lower compressive strength. Voids in the samples may be related to air bubbles during geopolymerization. it can be remarked also microcracks

are caused by fractures or delayed geopolymerization attributed to either slow activation in the early ages due to low alkali levels, rapid activation in the early ages or initial conditions (curing time and temperature). The unreacted FA particles in the samples reduce the compressive, their presence can be attributed to the incomplete geopolymerization. Samples cured at room temperature contain more unreacted FA particles, which can be explained by the slow dissolution and precipitation steps of the geopolymerization process (Mo et al., 2014).

GP9:

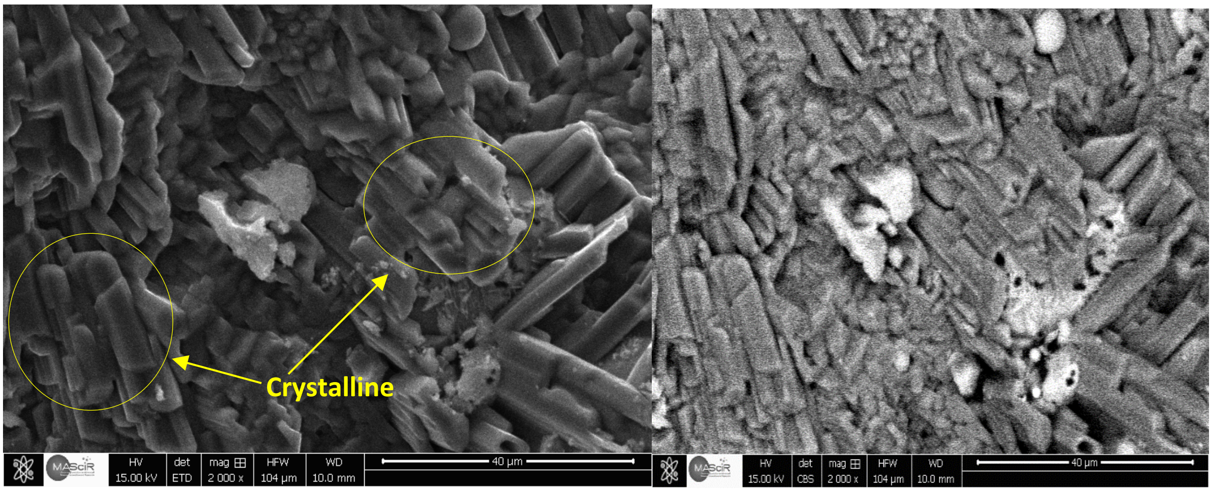


GP4 :

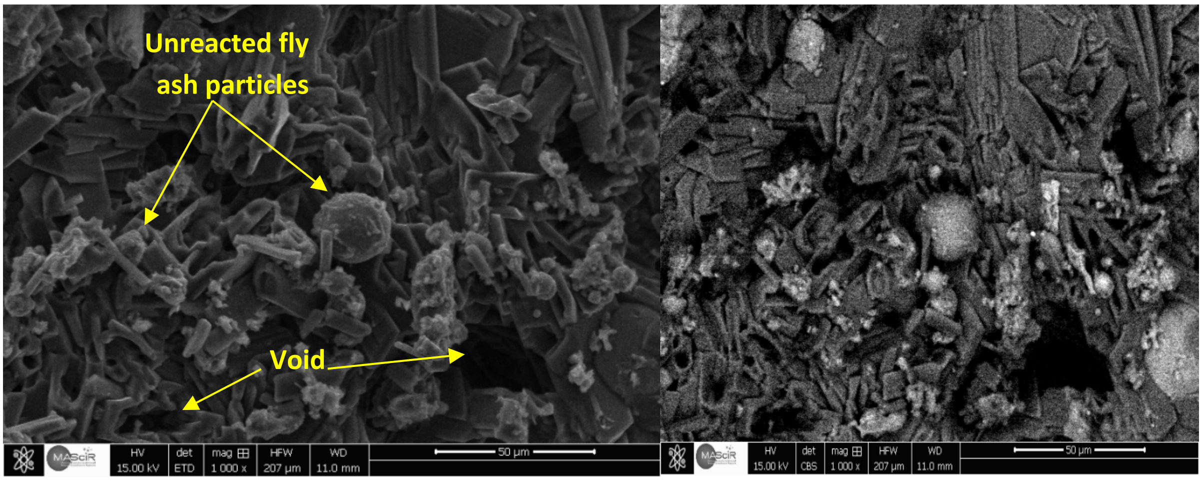


**Fig. 6: Micrographs SEM of geopolymers GP9 and GP4**

### 3.2 Statistical analysis

- **ANOVA**

**Table 7** presents the results of the analysis of variance, which reveals that as the probability of significance of the p-value risk is less than 0.05 (0.0383), the main effect of the regression is significant. The table also shows that the two factors curing time and curing temperature are the most significant.

**Table 7: Table of analysis of variance**

| Source | DL | Sum of Squares | CM | F | P |
|---|---|---|---|---|---|
| Regression | 6 | 41,935933 | 6,98932 | 25,4394 | 0,0383* |
| Residual | 2 | 0,5495 | 0,2747 | | |

| Total | 8 | 42,4854 | | |
|---|---|---|---|---|

- **Coefficient Effects Test**

The effect data for all the factors studied, as well as the statistical values of the t-student and the observed probability (p-value) are reported in **Table 8**. According to the table, the statistically significant coefficients are the linear terms $b_1$ and $b_2$.

**Table 8: Effects of model coefficients that relate response to factors**

| Source | degree of liberty | Sum of squares | Report F | Prob. > F |
|---|---|---|---|---|
| Curing time | 2 | 20,489622 | 37,2885 | 0,0261* |
| Curing Temperature | 2 | 18,449356 | 33,5755 | 0,0289* |
| Alkaline Solution | 2 | 2,996956 | 5,4541 | 0,1549 |

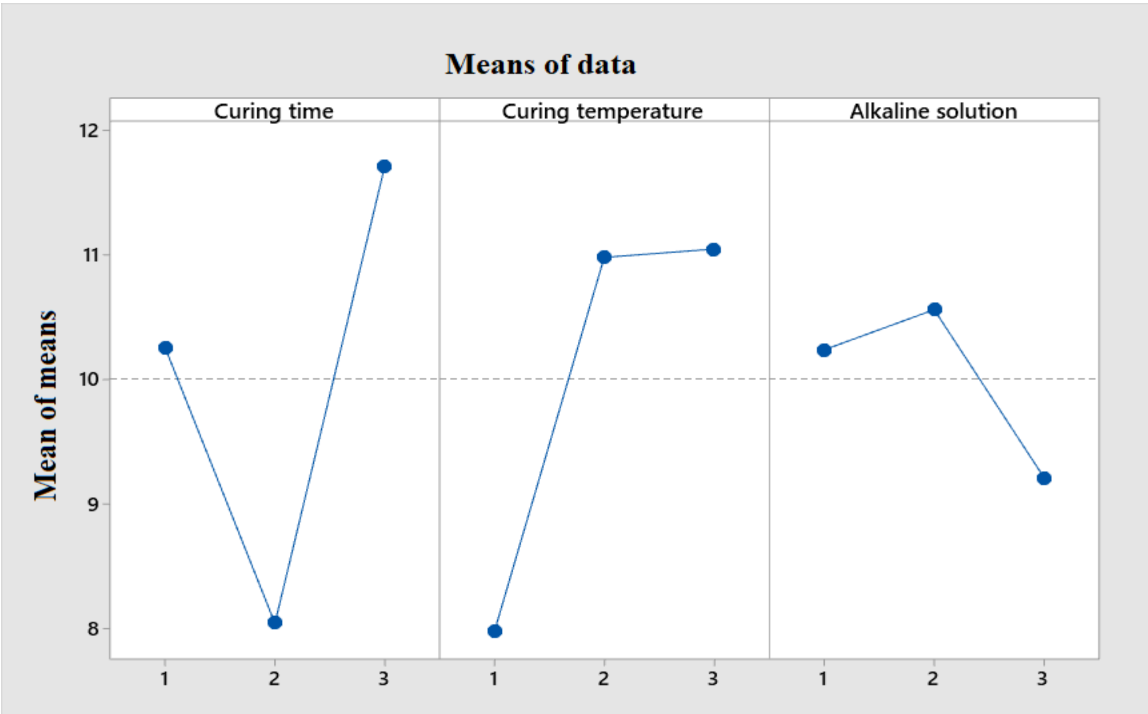


**Fig. 7: Graphics of the main effects**

The effect of curing time, temperature and the alkaline solution content on the response (compressive strength) is shown in **Fig. 7**. The study of curing time effect on the compressive strength indicated that the increase of this factor from 8 h to 12 h induces a decrease in response. However, a significant increase in reaching the maximum is observed at the 24 h curing time. The extension of the hardening time (up to 24 hours) seems to activate the geopolymerization process, thus leading to the densification of the geopolymer structure (Mo et al., 2014) and to the improvement of mechanical resistance. Criado et al stated that hardening time is an essential factor in the development of mechanical strengths as a result of the formation of an N-A-S-H alumino-silicate gel, which is richer in silicon (Criado et al., 2010). **Fig. 7** shows also that the oven curing temperature has a positive impact

on the mechanical strengths. The highest resistance is obtained for the temperature of 70°C and the lowest resistance is obtained at the temperature of 25°C (level 1). The reason for this phenomenon is that the geopolymerization reaction is slow at 25°C due to the low solubility of the aluminosilicate precursor. At higher temperatures (40-70°C), the solubility increases and a large amount of alumina and silica monomers are produced, thus accelerating the geopolymerization reaction as well as the production of the aluminosilicate gel responsible for the densification of the geopolymer matrix which leads to an improvement of the mechanical resistance (Davidovits, 2008; Mo *et al*., 2014). In some studies, the increase of the curing temperature above 75°C has been shown to have a negative impact on the strengths (Nazari *et al*., 2012), while in other studies it has been found that the increased temperature up to 90 ° C increases compressive strength (Riahi *et al*., 2012). Skvara et al (Škvára *et al*., 2005) have found that the maximum strengths are obtained for curing temperatures in the range 60-80 ° C with a curing time between 6-12 hours.

Besides that, the samples prepared using a mix of NaOH and KOH (level 2) showed the highest response (compressive strength). The geopolymer specimens using NaOH (level 1) as an alkaline activator has shown a higher response than that observed for KOH (level 3). The same results have been reported in the literature and explained by the fact that the ionic radius of $Na^+$ is smaller than that of the $K^+$ ion. Indeed, the small size of $Na^+$ effectively contributes to the activation of the dissolution step in the geopolymerization reaction, leading to the densification of the geopolymer matrix (van Jaarsveld *et al*., 2003; Xu and Van Deventer, 2000). $Na^+$ ions are strongly hydrated than $K^+$ due to the higher charge density of the former (Wijnen *et al*., 1990), and this liberates larger amounts of energy (390 kJ / mol for $Na^+$, compared to 305 kJ/mol for $K^+$) (Peng *et al*., 2015). This affects the rate of dissolution of silica because it depends on the degree of cationic hydration. The presence of NaOH improves the dissociation of Si and AL compared to KOH because Na $^+$ coagulates with monomeric silicates. The main reason is that it is easier to form more products and consequently a higher strength as observed here for NaOH activated systems (Phair and Van Deventer, 2002). on the other hand, K improves polycondensation because it has a larger unhydrated size and a lower charge density that favors the stabilization of silicate and aluminosilicate anions (Peng et al., 2015). The high compressive strength of the sample with Na/K is due to the influence of the presence of $K^+$ and $Na^+$ on the different stages of the geopolymerization reaction. The higher compressive strengths obtained for the 50% KOH and 50% NaOH mixture are due to the combined effect of $K^+$ and $Na^+$ ions.

**Table 9: The percentage of contribution of each factor on the compressive strength**

| *Curing time* | *Curing temperature* | *Alkaline solution* |
|---|---|---|
| **48,23 (%)** | **43,43 (%)** | **7,05 (%)** |
| Error percentage : **1,29%** | | |

**Table 10: The optimal conditions and the maximum response**

| **Curing time** | **Curing temperature** | **Alkaline solution** | **Maximum Predicted Response** |
|---|---|---|---|
| **24** | **70** | **50%NaOH** | **13,32** |

**Table 9** reports the contribution of each factor to the compressive strength and **Table 10** summarizes the optimal design conditions. The effects of curing time and temperature on the compressive strength are shown in **Table 8**; the curing time of 24 hours and temperature of 70°C have the maximum effect on the increase of compressive strength. In fact, the results obtained are consistent with those obtained by the works of Olivia & Nikraz (Olivia and Nikraz, 2012), Mijarsh *et al* (Mijarsh *et al*., 2014), Abdulkareem *et al* (Abdulkareem and Ramli, 2015) and Onoue *et al* (Onoue *et al*., 2019) where the maximum strength was obtained at high curing. temperature (around 70-75°C) and long curing time (24h and 48h).

In the present study, the use of a mixture of NaOH and KOH allowed us to obtain optimal compressive strength. Previous studies using NaOH have shown the best results but in our study, the role of the alkaline solution was the lowest compared to the curing time and temperature. The percentage of participation in the alkaline solution content is 7%.

## 4. Conclusion

In this work, Taguchi's method was used to study the effects of alkaline activator, curing time and temperature on the mechanical properties of GP based on FA class C. It was observed that the higher compressive strength was obtained for the sample formulated with an alkaline solution in the form of a mixture of Na and K at a curing temperature and time of 70 ° C and time of 24 h respectively. According to statistical analysis, the curing time and temperature influence the compressive strengths. The maximum compressive strength is obtained for a curing time of 24 hours and a temperature of 70 ° C. This fact is due to the increase in the rate of geopolymerization reaction by activating the dissolution and condensation steps. The low values of the mechanical strengths obtained can be improved by introducing organic and inorganic reinforcements, which will be the subject of our future works.

**Acknowledgement:** The authors would like to thank the Moroccan foundation for Advanced Science Innovation and Research (MaScIR) for conducting the SEM analyses

**Disclosure statement:** *Conflict of Interest:* The authors declare that there are no conflicts of interest.
*Compliance with Ethical Standards:* This article does not contain any studies involving human or animal subjects.

## References

Abdul Rahim R.H., Rahmiati T., Azizli K.A., Man Z., Nuruddin M.F., Ismail L. (2014). Comparison of Using NaOH and KOH Activated Fly Ash-Based Geopolymer on the Mechanical Properties. *Mater. Sci. Forum*., 803, 179–184. https://doi.org/10.4028/www.scientific.net/MSF.803.179

Abdulkareem O.A., Ramli M. (2015). Optimization of Alkaline Activator Mixing and Curing Conditions for A fly Ash-Based Geopolymer Paste System. *Mod. Appl. Sci.*, 9, 61. https://doi.org/10.5539/mas.v9n12p61

Alehyen, S., Achouri M.E., Taibi M., 2017. Characterization , microstructure and properties of fly ash-based geopolymer. *J. Mater. Environ. Sci.,* 8, 1783–1796.

Alouani M.E., Alehyen S., M. EL Achouri M. Taibi M. (2019). Elaboration of Inorganic Polymer for Removal of Organic Compound by Dynamic Column Test. *Mor. J. Chem.,* 7, 7–016. https://doi.org/10.48317/IMIST.PRSM/morjchem-v7i1.13890

Assi L.N., Eddie Deaver, E., Ziehl, P., 2018. Effect of source and particle size distribution on the mechanical and microstructural properties of fly Ash-Based geopolymer concrete. *Constr. Build. Mater.,* 167, 372–380. https://doi.org/10.1016/j.conbuildmat.2018.01.193

Bouguermouh K., Bouzidi, N., Mahtout, L., Rossignol, S., (2017). Synthesis, spectroscopic and mechanical properties of K and (K, Na)- geopolymers based on Algerian clays. *J. Mater. Environ. Sci.,* 8, 2203–2212.

Criado M., Fernández-Jiménez, A., Palomo, A., (2010). Alkali activation of fly ash. Part III: Effect of curing conditions on reaction and its graphical description. *Fuel.*, 89, 3185–3192. https://doi.org/10.1016/j.fuel.2010.03.051

Criado M., Palomo, A., Fernandezjimenez, A., (2005). Alkali activation of fly ashes. Part 1: Effect of curing conditions on the carbonation of the reaction products. *Fuel.*, 84, 2048–2054. https://doi.org/10.1016/j.fuel.2005.03.030

Davidovits J., (2008). Geopolymer Chemistry and Applications. ISBN: 9782954453118 5th edition, March 2020. Published by: Institut Géopolymère, Saint-Quentin France Web: www.geopolymer.org

de Vargas A.S., Dal Molin D.C.C., Vilela A.C.F., Silva F.J. da, Pavão B., Veit H. (2011). The effects of $Na_2O/SiO_2$ molar ratio, curing temperature and age on compressive strength, morphology and microstructure of alkali-activated fly ash-based geopolymers. *Cem. Concr. Compos.*, 33, 653–660. https://doi.org/10.1016/j.cemconcomp.2011.03.006

Fadil M., Fikri-Benbrahim K., Rachiq S., Ihssane B., Lebrazi S., Chraibi M., Haloui T., Farah A. (2018). Combined treatment of Thymus vulgaris L., Rosmarinus officinalis L. and Myrtus communis L. essential oils against Salmonella typhimurium : Optimization of antibacterial activity by mixture design methodology. *Eur. J. Pharm. Biopharm.,* 126, 211–220. https://doi.org/10.1016/j.ejpb.2017.06.002

Fletcher R.A., MacKenzie K.J.D., Nicholson C.L., Shimada S. (2005). The composition range of aluminosilicate geopolymers. *J. Eur. Ceram. Soc.*, 25, 1471–1477. doi.org/10.1016/j.jeurceramsoc.2004.06.001

Görhan G., Kürklü G., (2014). The influence of the NaOH solution on the properties of the fly ash-based geopolymer mortar cured at different temperatures. *Compos. Part B Eng.,* 58, 371–377. https://doi.org/10.1016/j.compositesb.2013.10.082

Hadi M.N.S., Farhan N.A., Sheikh M.N., (2017). Design of geopolymer concrete with GGBFS at ambient curing condition using Taguchi method. *Constr. Build. Mater.*, 140, 424–431. https://doi.org/10.1016/j.conbuildmat.2017.02.131

Hadrami A.E., Ojala S., Chatir E.M., Assaoui J., Bbrahmi R., (2020). Structural evolution and impact on the compressive strength of fly ash-based geopolymers. *Mor. J. Chem.*, 8, 8–626. https://doi.org/10.48317/IMIST.PRSM/morjchem-v8i3.20961

Hamidi, R.M., Man Z., Azizli K.A., (2016. Concentration of NaOH and the Effect on the Properties of Fly Ash Based Geopolymer. *Procedia Eng.*, 148, 189–193. https://doi.org/10.1016/j.proeng.2016.06.568

Hardjito, D., Cheak C.C., Lee Ing, C.H., (2008). Strength and Setting Times of Low Calcium Fly Ash-based Geopolymer Mortar. *Mod. Appl. Sci.,* 2, p3. https://doi.org/10.5539/mas.v2n4p3

Hardjito D., Wallah S., Rangan, B., (2002). Study on engineering properties of fly ash-based geopolymer concrete. *J. Australas. Ceram. Soc.,* 38, 44–47.

Hardjito D., Wallah S.E., Sumajouw D.M.J., Rangan B.V., (2004). On the Development of Fly Ash-Based Geopolymer Concrete. *ACI Mater.,* J. 6.

Hosan A., Haque S., Shaikh, F., (2016). Compressive behaviour of sodium and potassium activators synthetized fly ash geopolymer at elevated temperatures: A comparative study. *J. Build. Eng.,* 8, 123–130. https://doi.org/10.1016/j.jobe.2016.10.005

Kaur K., Singh J., Kaur M., (2018). Compressive strength of rice husk ash based geopolymer: The effect of alkaline activator. *Constr. Build. Mater.*, 169, 188–192. https://doi.org/10.1016/j.conbuildmat.2018.02.200

Lee W.K.W., van Deventer, J.S.J., (2002). The effects of inorganic salt contamination on the strength and durability of geopolymers. *Colloids Surf. Physicochem. Eng. Asp.*, 211, 115–126. https://doi.org/10.1016/S0927-7757(02)00239-X

Leong H.Y., Ong, D.E.L., Sanjayan, J.G., Nazari, A., (2016). The effect of different Na 2 O and K 2 O ratios of alkali activator on compressive strength of fly ash based-geopolymer. *Constr. Build. Mater.*, 106, 500–511. https://doi.org/10.1016/j.conbuildmat.2015.12.141

Mijarsh M.J.A., Megat Johari, M.A., Ahmad, Z.A., (2014). Synthesis of geopolymer from large amounts of treated palm oil fuel ash: Application of the Taguchi method in investigating the main parameters affecting compressive strength. *Constr. Build. Mater.*, 52, 473–481. doi.org/10.1016/j.conbuildmat.2013.11.039

Mo B., Zhu, H., Cui, X., He, Y., Gong, S., (2014. Effect of curing temperature on geopolymerization of metakaolin-based geopolymers. *Appl. Clay Sci.*, 99, 144–148. doi.org/10.1016/j.clay.2014.06.024

Monsif M., Rossignol, S., Fouzia, A., Zerouale, A., Kandri, N., Joussein, E., Tamburini, S., Bertani, R., 2017. The implementation of geopolymers materials from Moroccan clay, within the framework of the valorization of the local natural resources. *J. Mater. Environ. Sci.*, 8, 2701–2721.

Moutaoukil G., Alehyen, S., Sobrados, I., Taibi, M., 2022. Microstructural and 29Si and 27Al MAS NMR spectroscopic evaluations of alkali cation and curing effects on Class C fly ash-based geopolymer. *Chem. Data Collect.,* 41, 100898. https://doi.org/10.1016/j.cdc.2022.100898

Nazari A., Bagheri A., Riahi, S. (2011). Properties of geopolymer with seeded fly ash and rice husk bark ash. *Mater. Sci. Eng.*, A 528, 7395–7401. https://doi.org/10.1016/j.msea.2011.06.027

Nazari A., Khanmohammadi H., Amini M., Hajiallahyari H., Rahimi A. (2012). Production geopolymers by Portland cement: Designing the main parameters' effects on compressive strength by Taguchi method. *Mater. Des.*, 41, 43–49. https://doi.org/10.1016/j.matdes.2012.04.045

Nmiri A., Duc M., Hamdi N., yazoghli O., Srasra E. (2017). Alkaline activation effect on calcined kaolinitic clay at different temperatures. *J. Mater. Environ. Sci.,* 8, 676–690.

Olivia M., Nikraz H., 2012. Properties of fly ash geopolymer concrete designed by Taguchi method. *Mater. Des.,* 1980-2015 36, 191–198. https://doi.org/10.1016/j.matdes.2011.10.036

Onoue K., Iwamoto T., Sagawa Y. (2019). Optimization of the design parameters of fly ash-based geopolymer using the dynamic approach of the Taguchi method. *Constr. Build. Mater.,* 219, 1–10. https://doi.org/10.1016/j.conbuildmat.2019.05.177

Palomo A., Blanco-Varela M.T., Granizo M.L., Puertas F., Vazquez, T., Grutzeck, M.W. (1999). Chemical stability of cementitious materials based on metakaolin. *Cem. Concr. Res.,* 29, 997–1004. https://doi.org/10.1016/s0008-8846(99)00074-5

Peng Z., Vance K., Dakhane, A., Marzke, R., Neithalath, N. (2015). Microstructural and 29Si MAS NMR spectroscopic evaluations of alkali cationic effects on fly ash activation. *Cem. Concr. Compos.,* 57, 34–43. https://doi.org/10.1016/j.cemconcomp.2014.12.005

Phair J.W., Van Deventer J.S.J. (2002). Effect of the silicate activator pH on the microstructural characteristics of waste-based geopolymers. *Int. J. Miner. Process.*, 66, 121–143. https://doi.org/10.1016/s0301-7516(02)00013-3

Rattanasak U., Chindaprasirt P. (2009). Influence of NaOH solution on the synthesis of fly ash geopolymer. *Miner. Eng.,* 22, 1073–1078. https://doi.org/10.1016/j.mineng.2009.03.022

Riahi S., Nazari A., Zaarei D., Khalaj G., Bohlooli H., Kaykha M.M. (2012). Compressive strength of ash-based geopolymers at early ages designed by Taguchi method. *Mater. Des.*, 37, 443–449. https://doi.org/10.1016/j.matdes.2012.01.030

Siyal A.A., Azizli K.A., Man Z., Ullah H. (2016). Effects of Parameters on the Setting Time of Fly Ash Based Geopolymers Using Taguchi Method. *Procedia Eng.*, 148, 302–307. https://doi.org/10.1016/j.proeng.2016.06.624

Škvára F., Jílek, T., Kopecky, L., (2005. Geopolymer Materials Based on Fly Ash. *Ceram. - Silik.*, 49, 195–204.

Škvára F., Kopecky, L., Myskova, L., Šmilauer, V., Alberovská, L., Vinšová, L., 2009). Aluminosilicate polymers - Influence of elevated temperatures, efflorescence. *Ceram. - Silik.,* 53, 276–282.

Soutsos M., Boyle, A.P., Vinai, R., Hadjierakleous, A., Barnett, S.J., (2016). Factors influencing the compressive strength of fly ash based geopolymers. *Constr. Build. Mater.*, 110, 355–368. https://doi.org/10.1016/j.conbuildmat.2015.11.045

Temuujin J., Williams, R.P., van Riessen A. (2009). Effect of mechanical activation of fly ash on the properties of geopolymer cured at ambient temperature. *J. Mater. Process. Technol.,* 209, 5276–5280. https://doi.org/10.1016/j.jmatprotec.2009.03.016

Türkmen İ., Gül, R., Çelik C. (2008). A Taguchi approach for investigation of some physical properties of concrete produced from mineral admixtures. *Build. Environ.*, 43, 1127–1137. https://doi.org/10.1016/j.buildenv.2007.02.005

van Jaarsveld J.G.S., van Deventer J.S.J. (1999). Effect of the Alkali Metal Activator on the Properties of Fly Ash-Based Geopolymers. *Ind. Eng. Chem. Res.*, 38, 3932–3941. https://doi.org/10.1021/ie980804b

van Jaarsveld J.G.S., van Deventer J.S.J., Lukey G.C. (2003). The characterisation of source materials in fly ash-based geopolymers. *Mater. Lett.*, 57, 1272–1280. https://doi.org/10.1016/S0167-577X(02)00971-0

van Jaarsveld J.G.S., van Deventer J.S.J., Lukey G.C.(2002). The effect of composition and temperature on the properties of fly ash- and kaolinite-based geopolymers. *Chem. Eng. J.,* 89, 63–73. https://doi.org/10.1016/S1385-8947(02)00025-6

Wijnen P.W.J.G., Beelen T.P.M., De Haan J.W., Van De Ven L.J.M., Van Santen R.A. (1990). The structure directing effect of cations in aqueous silicate solutions. A 29Si-NMR study. *Colloids Surf.,* 45, 255–268. https://doi.org/10.1016/0166-6622(90)80029-4

Xu H., van Deventer J.S.J. (2003). The effect of alkali metals on the formation of geopolymeric gels from alkali-feldspars. *Colloids Surf. Physicochem. Eng. Asp.,* 216, 27–44. https://doi.org/10.1016/S0927-7757(02)00499-5

Xu H., Van Deventer J.S.J. (2000). The geopolymerisation of alumino-silicate minerals. *Int. J. Miner. Process.*, 59, 247–266. https://doi.org/10.1016/S0301-7516(99)00074-5

Xu H., van Deventer, J.S.J., Lukey G.C., (2001). Effect of Alkali Metals on the Preferential Geopolymerization of Stilbite/Kaolinite Mixtures. *Ind. Eng. Chem. Res*., 40, 3749–3756. https://doi.org/10.1021/ie010042b

Yao X., Zhang, Z., Zhu, H., Chen Y. (2009). Geopolymerization process of alkali–metakaolinite characterized by isothermal calorimetry. *Thermochim. Acta.,* 493, 49–54. https://doi.org/10.1016/j.tca.2009.04.002

Zhang Z., Wang, H., Provis J.L. (2012). Quantitative study of the reactivity of fly ash in geopolymerization by FTIR. *J. Sustain. Cem.-Based Mater.,* 1, 154–166. https://doi.org/10.1080/21650373.2012.752620

(2023) ; https://revues.imist.ma/index.php/morjchem/index